A Broadband Graphene-Based THz Coupler with Wide-Range Tunable Power-Dividing Ratios

Yongle Wu[1,a)], Meijun Qu[2,b)], Yuanan Liu[1], and Z. Ghassemlooy[3]

[1]School of Electronic Engineering, Beijing Key Laboratory of Work Safety Intelligent Monitoring, Beijing University of Posts and Telecommunications, P. O. Box. 282, Beijing, 100876, China.

[2]School of Information and Communication Engineering, Beijing Key Laboratory of Network System Architecture and Convergence, Beijing University of Posts and Telecommunications, Beijing, 100876, China.

[3]Optical Communications Research Group, NCRLab, Faculty of Engineering and Environment, Northumbria University, Newcastle upon Tyne, NE1 8ST, U.K.

Contents

Abstract 1
Introduction 2
Graphene-based THz broadband coupler design 2
Parameters analysis of the proposed graphene-based coupler 3
Results and discussions 6
Conclusions 8
References 9

Abstract: A wideband coupler based on the graphene with inherent DC-block function and adjustable power-dividing ratios is proposed. This coupler uses three sections of the two-line coupled lines, four sections of the three-line coupled lines and four graphene stubs (two U-shaped stubs and two rectangular stubs). The graphene stubs allow the coupler to own dynamic surface conductivity, which could be tuned by altering the chemical potentials. The tunable power-dividing ratios could be achieved by varying the chemical potentials applied to the U-shaped graphene stubs and the rectangular graphene elements, respectively. In addition, the widths of two-line coupled lines in the proposed coupler are analyzed to affect the power-dividing ratios in detail. Finally, the power-dividing ratios of the proposed coupler have a variation range from 5.4 dB to 9.56 dB at 1.75 THz with a flat 90° phase shift. The minimum -10 dB impedance bandwidth is 44 % from 1.47 THz to 2.3 THz, thus indicating a wide-band performance.

Key words: wide-band, coupler, adjustable power-dividing ratios, graphene.

[a]Yongle Wu and [b]Meijun Qu contributed equally to this work.
[a]wuyongle138@gmail.com.

I. Introduction

The graphene technology has attracted growing attention due to its potential in nano-electronics and nano-photonics devices [1-4]. One key feature is that the surface complex conductivity can be easily controlled by varying the applied chemical potential. The use of graphene also facilitates designing a range of devices and antennas with adjustable features [5-7]. For example, the tunable features of the bandwidth reconfigurable uniplanar coplanar waveguide (strip) power divider [5], the Yagi-Uda antenna with reconfigurable radiation patterns [6], and the tunable filter-integrated quasi-Yagi antenna [7] have been achieved by using graphene. Nowadays, the wide-band microwave or terra Hertz (THz) couplers with dissimilar power-dividing ratios (PDRs) have attracted growing interests. These devices can be applied in the feeding network of microwave/THz antennas, antenna arrays, mixers, and power amplifiers, to name a few. However, there are no reports on a wide-band THz coupler with tunable PDRs capability.

This paper reports for the first time a novel broadband graphene-based THz coupler with wide-range tunable PDRs. The proposed THz coupler is constructed by combining the basic circuit layout of the filter-integrated coupler in [8] and four additional graphene stubs. The PDRs can be changed by altering the chemical potentials applied to the four graphene stubs. Five simulated cases are illustrated to validate our proposed idea. From the demonstrated results, it can be observed that the graphene-based THz coupler has a number of advantages including compact size, broadband operation, excellent adjustable PDRs, flat phase shift, and an inherent DC-blocking feature between the two arbitrary output ports.

II. Design of Graphene-based THz broadband coupler

Figs.1 (a) and (b) show the top and side views of the proposed graphene-based broadband THz coupler with the geometrical parameters. It consists of three sections of two-line coupled lines, four sections of three-line coupled lines and four graphene stubs (shown as black sections). μ_c represents the chemical potential applied to the graphene stubs. μ_{c1} and μ_{c2} are the chemical potentials applied to the two U-shaped elements and two rectangular stubs, respectively. It should be mentioned that the technology of hybrid graphene-metal implementation has been demonstrated experimentally in [9, 10]. The substrate is constructed based on SiO_2 with a dielectric constant of 3.8 and a thickness of 1μm. The proposed coupler is simulated using the full-wave electromagnetic simulator (ANSYS HFSS tool based on finite element method). The graphene can be modeled as a 2-D surface with complex conductivity σ in the full-wave simulator. The intra and inter conductivities defined by Kubo's formulas can be calculated by [5-7, 11, 12]

$$\sigma_{\text{intra}} \approx \frac{-je^2 k_B T}{\pi\hbar^2(\omega - j2\Gamma)}\left[\frac{\mu_c}{k_B T} + 2\ln\left(e^{-\mu_c/(k_B T)} + 1\right)\right], \tag{1}$$

$$\sigma_{\text{inter}} \approx \frac{-je^2}{4\pi\hbar}\ln\left(\frac{2|\mu_c| - (\omega - j2\Gamma)\hbar}{2|\mu_c| + (\omega - j2\Gamma)\hbar}\right), \tag{2}$$

where e is the electron charge, ω is the angular frequency, k_B is the Boltzmann constant, $\hbar$ is the reduced Plank constant, T is the temperature in Kelvin, τ is the electron relaxation time, and $\Gamma=1/(2\tau)$ is the electron scattering rate. T = 300 K and τ = 1 ps is assumed [13], and only the intra-band contribution is considered in this paper.

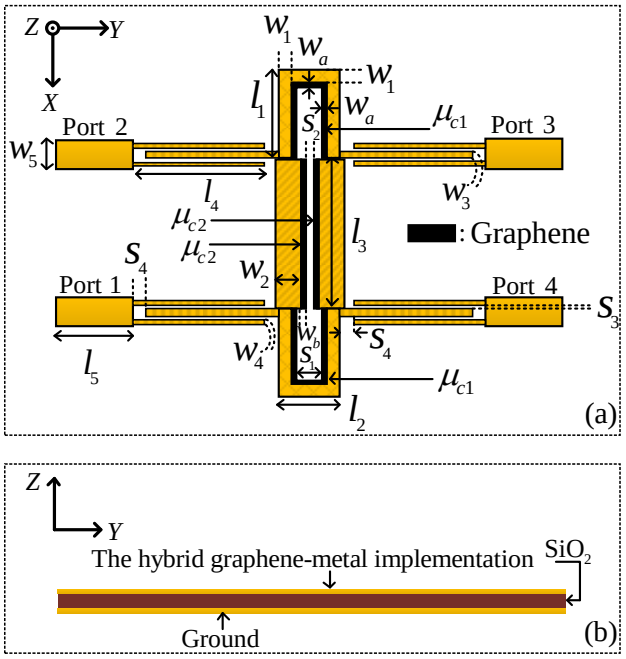

FIG. 1. Configuration of the proposed graphene-based broadband THz coupler with geometrical parameters: (a) top view, and (b) side view.

III. Parameters analysis of the proposed graphene-based coupler

According to the results in [8], the widths of two-line coupled lines are strongly related to the PDRs of this kind of coupler. In order to adjust the PDRs, four graphene stubs including two U-shaped stubs and two rectangular stubs are introduced in the interior of two-line coupled lines in the previous coupler. Thus, the dynamic PDRs can be achieved by varying the chemical potentials (i.e., μ_{c1} and μ_{c2}) applied to four inserted graphene stubs. The general geometrical parameters for the following analysis are listed in TABLE I.

TABLE I. The geometrical dimensions of the proposed grapheme-based THz broadband coupler

Parameters	Values (μm)	Parameters	Values (μm)
l_1	10	w_1	0.5
l_2	4.55	w_2	3.15
l_3	17	w_3	0.7
l_4	23	w_4	0.2
l_5	10	w_5	1.9
w_a	0.5	w_b	0.55
s_1	2.55	s_2	0.25
s_3	0.2	s_4	1.75

Although four graphene stubs are inserted in this proposed tunable coupler, the widths of two-line coupled lines (w_1 and w_2) have strong influence on the final PDRs, similar with the previous microwave coupler in [8]. As shown in Fig. 2, the PDR [dB($|S_{21}|$)- dB($|S_{31}|$)] decreases when the line width w_1 increases. This phenomenon exists in all four cases with different chemical potential μ_{c1}. Obviously, the matching and isolation performance is also affected by both the line width w_1 and the chemical potential μ_{c1}. Fig. 3 shows the performance variation with different values of the line width w_2 and the chemical potential μ_{c2}. Different from the phenomenon in Fig. 2, the PDR [dB($|S_{21}|$)- dB($|S_{31}|$)] increases with the increasing of the line width w_2. This increasing feature can be observed in all four cases with different chemical potential μ_{c2}. Another important difference between Fig.2 and Fig. 3 is that the PDR [dB($|S_{21}|$)- dB($|S_{31}|$)] in Fig.2 is more flatter than the one in Fig.3. Therefore, tuning the line width w_1 is preferred in designing or optimizing the desired PDR for this proposed tunable coupler.

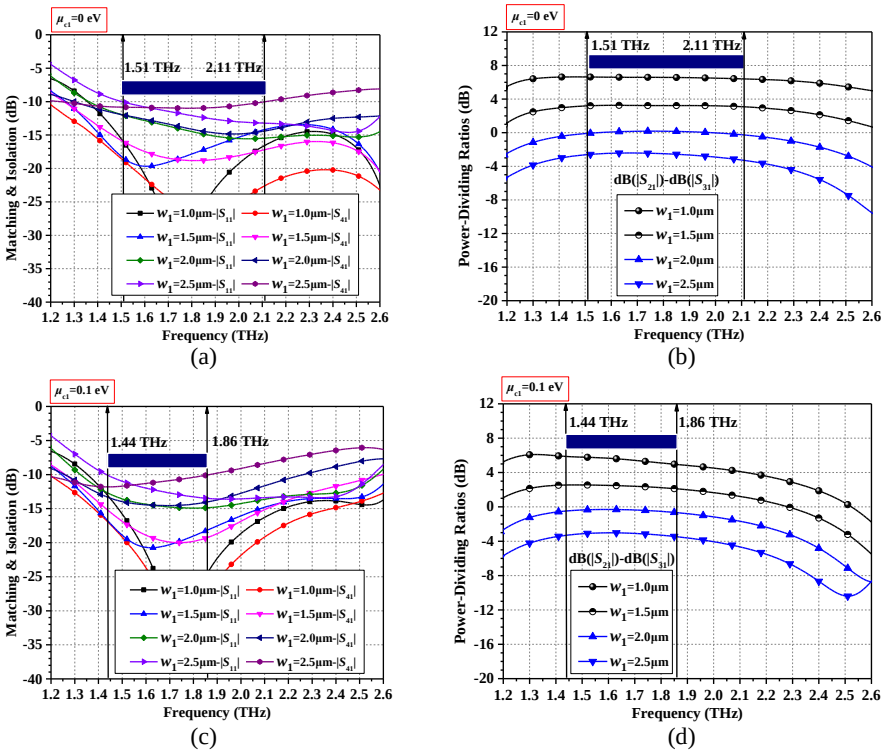

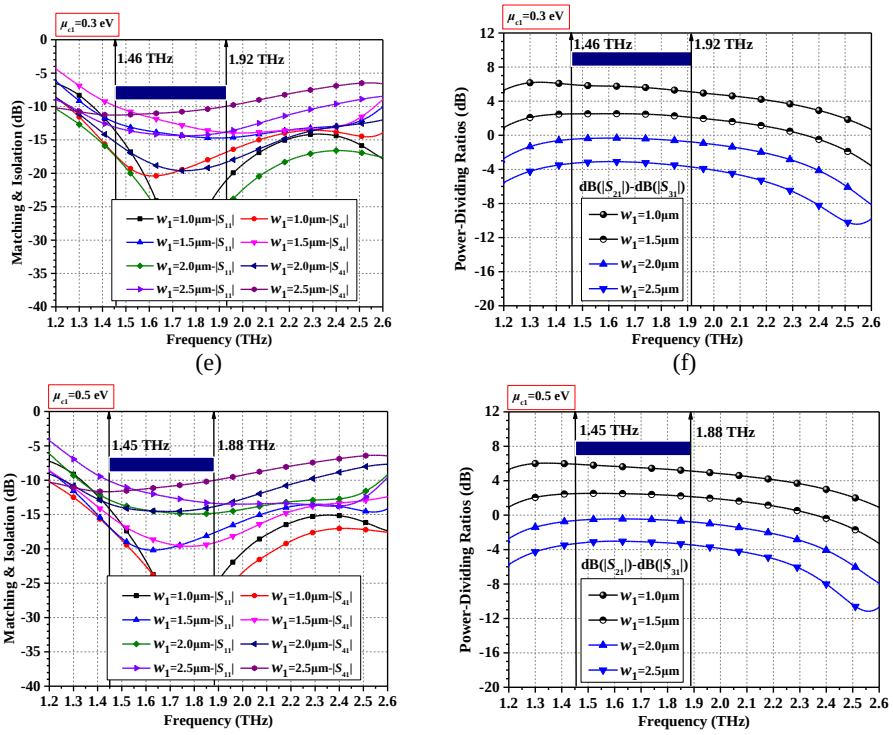

FIG. 2. The curves of matching, isolation, and power-dividing ratios (PDRs) when μ_{c2} is set to 0 eV, w_2 is 3.7 um, and μ_{c1}=0 eV (a, b), μ_{c1}=0.1 eV (c, d), μ_{c1}=0.3 eV (e, f), and μ_{c1}=0.5 eV (g, h), respectively. Other parameters are given in TABLE I.

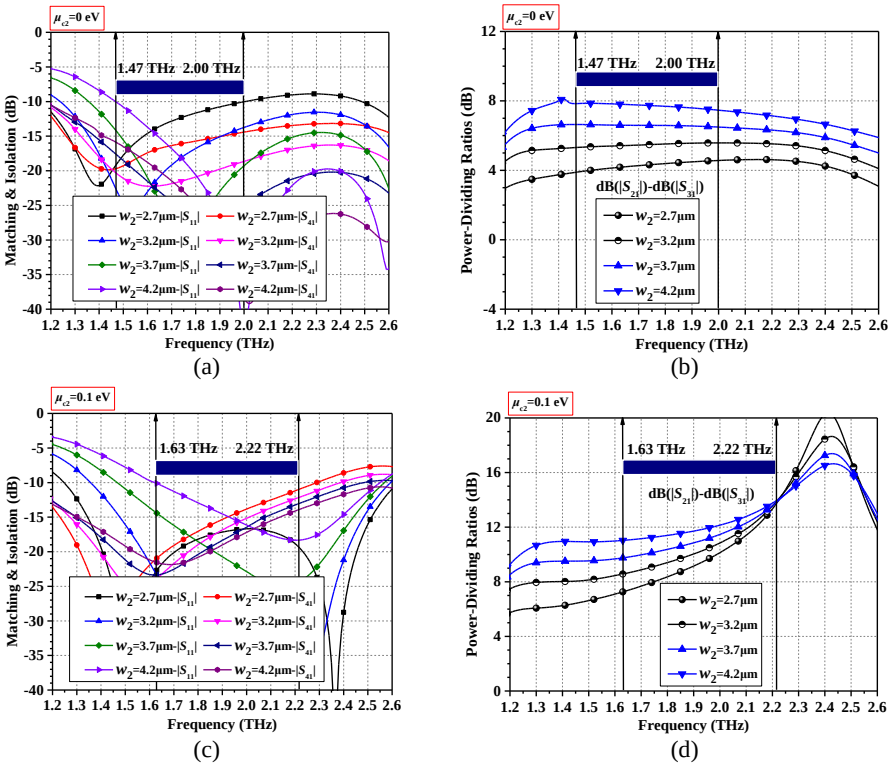

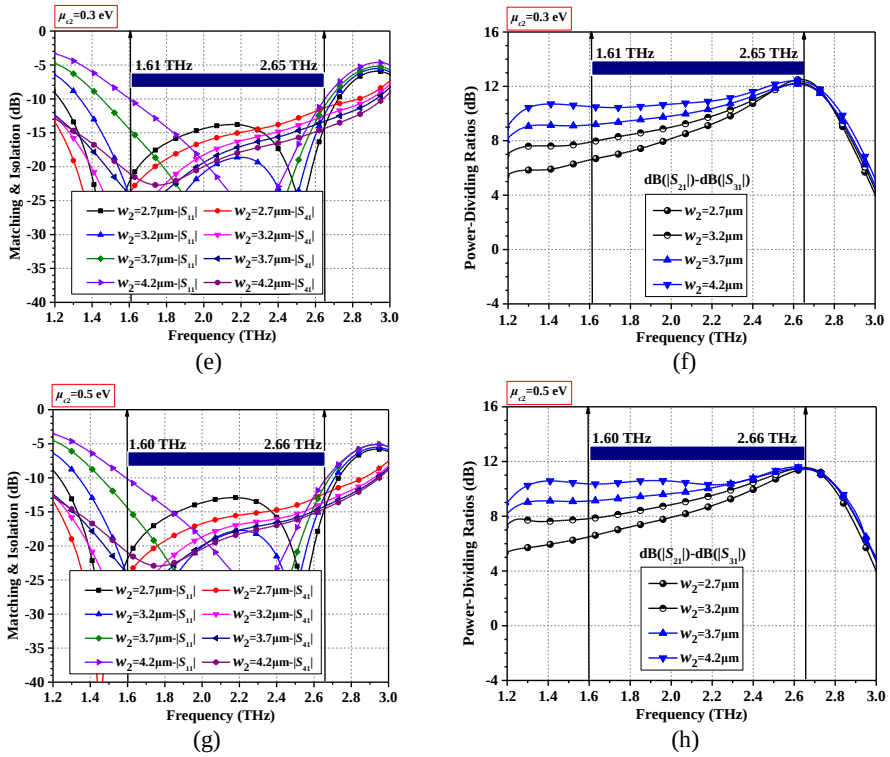

FIG. 3. The curves of matching, isolation, and power-dividing ratios (PDRs) when μ_{c1} is set to 0 eV, w_1 is 1 um, and μ_{c2}=0 eV (a, b), μ_{c2}=0.1 eV (c, d), μ_{c2}=0.3 eV (e, f), and μ_{c2}=0.5 eV (g, h), respectively. Other parameters are given in TABLE I.

IV. Results and discussions

The final THz couplers with five different PDRs are designed to verify the proposed idea (Case 1: μ_{c1} = 0.3 eV, μ_{c2} = 0 eV; Case 2: μ_{c1} = 0 eV, μ_{c2} = 0 eV; Case 3: μ_{c1} = 0.1 eV, μ_{c2} = 0.2 eV; Case 4: μ_{c1} = 0.1 eV, μ_{c2} = 0.1 eV; and Case 5: μ_{c1} = 0 eV, μ_{c2} = 0.2 eV). TABLE I lists the final parameters' values. Fig. 4 depicts the simulated results for operating characteristics of the proposed THz coupler for a range of PDRs. Fig. 4(a) illustrates the excellent matching and high isolation of the proposed coupler with the minimum -10 dB impedance bandwidth from 1.47 THz to 2.3 THz (44 %). Fig. 4(b) depicts the transmission and coupling characteristics showing five different coupling coefficients, which are obtained over the acceptable range of 1.47 THz to 2.3 THz. The phase difference profile showing a flat 90° phase shift and with the largest deviation of almost ±3.8° can be observed from the Fig. 4(c). Finally, Figs. 4(d) and 5 illustrate the PDRs for the Cases 1-5. Fig. 5 accurately displays the PDRs in terms of the quantitative values at 1.65 THz, 1.75 THz and 1.85 THz. The predicted PDRs for the Cases 1-5 are about 5.4, 6.6, 8, 8.46, 9.56 dB, respectively at 1.75 THz. It can be observed in Fig. 5 that the tendencies of these three curves are the same, and the values of PDRs are quite close in all the five cases, indicating a wide-band tunable PDRs function.

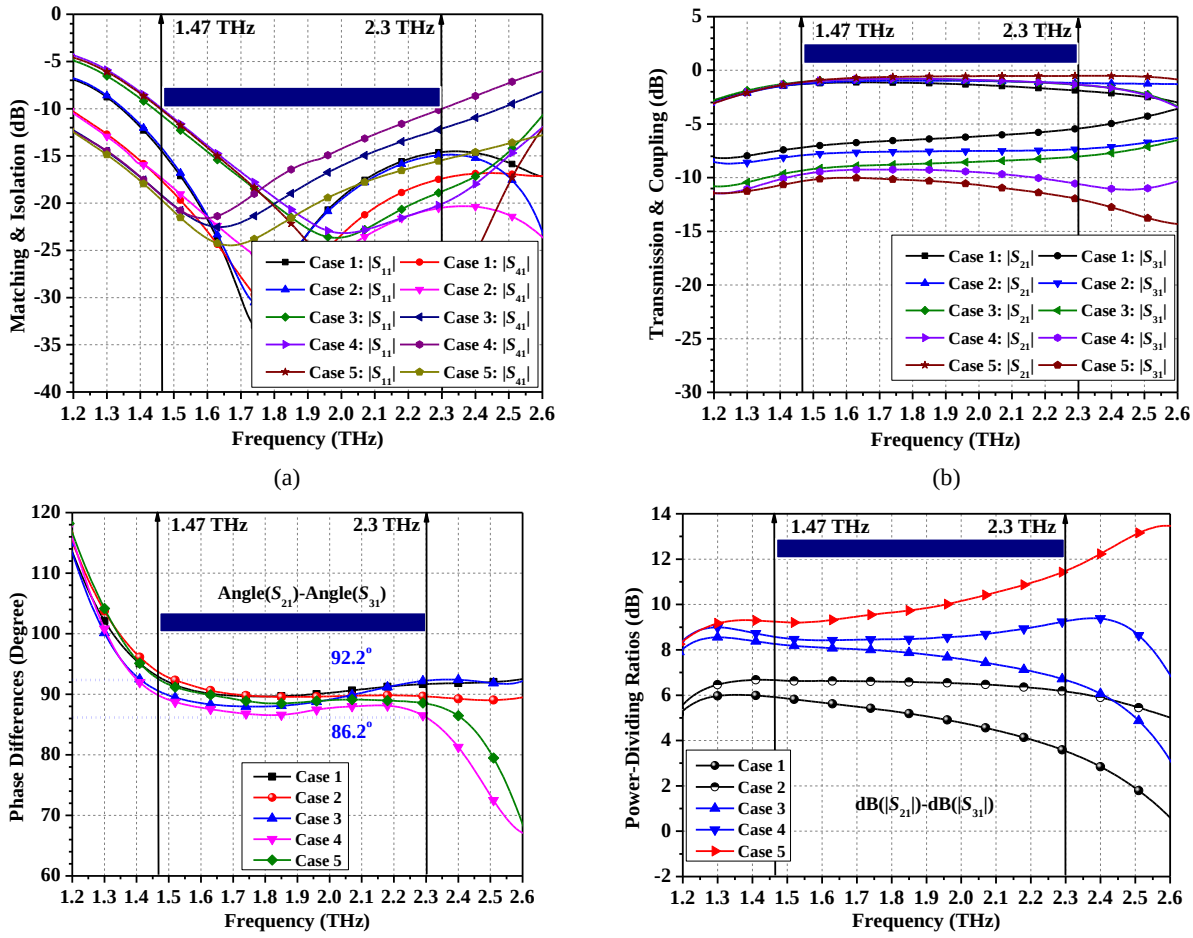

FIG. 4. The simulated results for the proposed THz coupler for: (a) matching and isolation, (b) transmission and coupling, (c) phase differences, and (d) tunable power-dividing ratios.

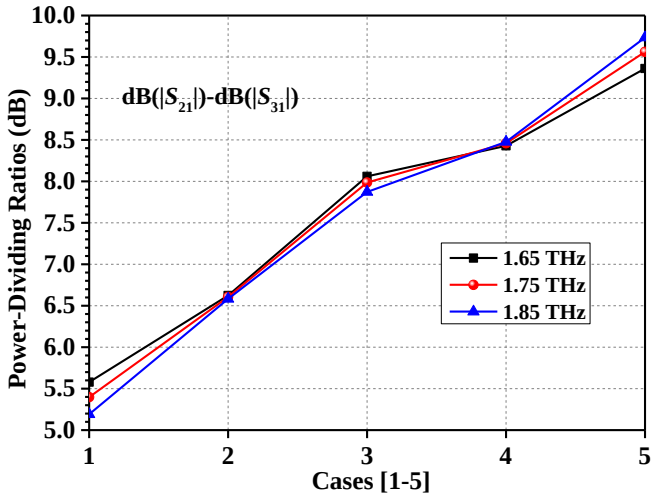

FIG. 5. The values of power-dividing ratios at 1.65 THz, 1.75 THz, and 1.85 THz in the proposed tunable coupler.

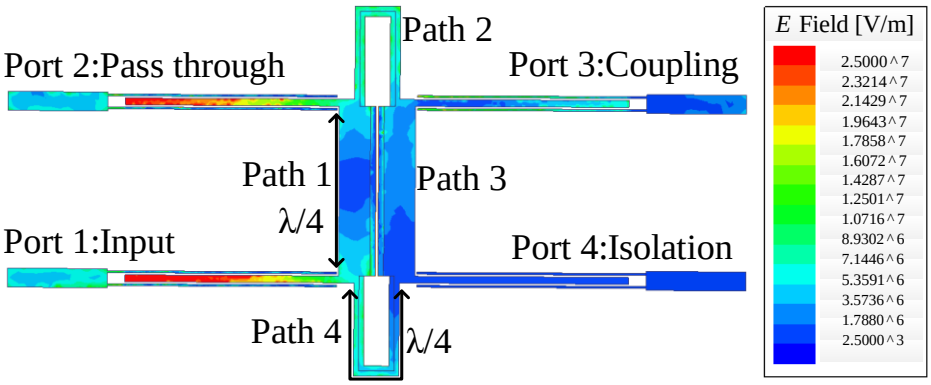

FIG. 6. The *E* field distributions in the proposed graphene-based tunable coupler with 5.4-dB PDR at 1.75 THz.

In order to explain the coupling mechanism of this proposed graphene-based tunable coupler, the electric *E* field distributions are presented in Fig. 6. It can be obtained from Fig. 6 that the electromagnetic energy from Port 1 is mainly transmitted to Port 2 while other smaller part of the electromagnetic energy is coupled to Port 3. Note that there is not any electromagnetic energy outputting from Port 4. The electrical lengths of Path 1, Path 2, Path 3, and Path 4 are about 90° at 1.75 THz. Therefore, the phase difference between Port 2 and Port 3 is almost 90°, and the corresponding electric *E* field distributions in Fig.6 can verify this phase-difference performance.

V. Conclusions

A broadband coupled-line THz coupler based on the graphene with wide-range tunable power-dividing ratios and a DC-blocking feature has been presented. The power-dividing ratio of the proposed THz coupler can readily be changed by altering the chemical potentials applied to the four graphene stubs (two U-shaped stubs and two rectangular stubs) without deteriorating the matching, isolation and phase-difference performances. In addition, the widths of two-line coupled lines in the graphene-based coupler are analyzed to affect the power-dividing ratios in detail. The simulated results show that this proposed coupler can achieve higher tunable power-dividing ratios from 5.4 dB to 9.56 dB at 1.75 THz with a flat 90° phase shift. The minimum -10 dB impedance bandwidth is 44 % from 1.47 THz to 2.3 THz, thus achieving the broadband operation.

Acknowledgments

This work was supported by National Basic Research Program of China (973 Program) (No. 2014CB339900), and National Natural Science Foundations of China (No.61422103, No.61671084, and No.61327806).

References

[1]M. Danaeifar, N. Granpayeh, A. Mohammadi, and A. Setayesh, Applied Optics, **52**(22), E68-E72 (2013).
[2]M. He, K. Wang, L. Wang, J. Li, J. Liu, Z. Huang, L. Wang, L. Wang, W. Hu, and X. Chen, Applied Physics Letters, **105** 081903:1-5 (2014).
[3]M. Tamagnone, J. S. Gómez-Díaz, J. R. Mosig, and J. Perruisseau-Carrier, Applied Physics Letters, **101**, 214102: 1-4 (2012).
[4]M. Tamagnone, J. S. Gómez-Díaz, J. R. Mosig, and J. Perruisseau-Carrier, Journal of Applied Physics, **112**, 114915:1-4 (2012).
[5]Y. Wu, M. Qu, and Y. Liu, Scientific Reports, DOI: 10.1038/srep31760:1-8 (2016).
[6]Y. Wu, M. Qu, L. Jiao, Y. Liu, and Z. Ghassemlooy, AIP Advances **6**, 065308:1-11(2016).
[7]Y. Wu, M. Qu, L. Jiao, and Y. Liu, Plasmonics, DOI: 10.1007/s11468-016-0328-9 (2016).
[8]Y. Wu, L. Jiao, Y. Du, and Y. Liu, Microwave and Optical Technology Letters, **58** (1), 121-123 (2016).
[9]L. Wang, I. Meric, P. Y. Huang, Q. Gao, Y. Gao, H. Tran, T. Taniguchi, K. Watanabe, L. M. Campos, D. A. Muller, J. Guo, P. Kim, J. Hone, K. L. Shepard, and C. R. Dean, Science, **342**(6158), 614-617 (2013).
[10]L. Pierantoni, D. Mencarelli, M. Bozzi, R. Moro, S. Moscato, L. Perregrini, F. Micciulla, A. Cataldo, and Stefano Bellucci, IEEE Transactions on Microwave Theory and Techniques, **63**(8), 2491-2497 (2015).
[11]G. Hanson, IEEE Transactions on Antennas and Propagation, **56** (3), 747-757 (2008).
[12]G. Hanson, Journal of Applied Physics, **104**, 084314: 1-5 (2008).
[13]D. Correas-Serrano, J. S. Gomez-Diaz, A. Alù, and A. Álvarez Melcón, IEEE Transactions on Terahertz Science and Technology, **5**(6), 951- 960 (2015).